Journal of the Korean Electrochemical Society
Vol. 4, No. 2, 2001, 70-76

총 설

Application of Laser Beam Deflection Technique to Analysis of Stresses Generated during Hydrogen Diffusion through Pd Foil Electrode

Jeong-Nam Han and Su-Il Pyun†

Corrosion and Interfacial Electrochemistry Research Laboratory at Department of Materials Science and Engineering, Korea Advanced Institute of Science and Technology, 373-1 Kusong-Dong, Yusong-Gu, Taejon 305-701, Korea
(Received February 26, 2001 : Accepted March 13, 2001)

Abstract. The present work describes the capabilities of laser beam deflection (LBD) technique for the analysis of the stresses developed during hydrogen diffusion through Pd foil electrode. First, we explain briefly the elasto-diffusive (Gorsky effect) and diffusion-elastic phenomena. A model for the diffusion-elastic phenomenon is theoretically derived from the solution of the Fick's equation for given initial and boundary conditions, Vegard's second law and Hooke's law. Second, we introduce how to apply the principle of LBD technique to the study on the stresses generated during hydrogen diffusion. From the comparison of the deflection transients numerically calculated with those experimentally measured, we finally discuss the change in the tensile deflection with time in terms of hydrogen concentration profile transient and hydrogen diffusivity.

초 록 : 본 연구는 Pd 박막 전극에서 수소 확산시 발생되는 응력해석에 대한 레이저 빔 디플렉션 방법의 응용에 대해 기술하였다. 우선, 탄성에 의한 확산 (고스키 효과) 및 확산에 의한 탄성 현상에 대해 간략히 설명하였고, 주어진 초기 및 경계 조건하에서 Fick 방정식의 해와 Vegard 및 Hooke의 법칙으로부터 확산에 의한 탄성 현상의 모델을 이론적으로 유도하였다. 다음으로 레이저 빔 디플렉션 방법이 수소 확산으로 인해 발생되는 응력해석에 어떻게 사용될 수 있는지 실험 장치 및 시편에 대해 소개하였다. 마지막으로, 수학적으로 계산된 디플렉션 시간 추이 곡선과 실험적으로 얻어진 곡선의 비교로부터, 시간에 따른 인장 디플렉션의 변화를 시간에 따른 전극 내부의 수소 농도 구배의 변화 및 수소 확산계수의 차이로 설명하였다.

Key words : Stress generation, Hydrogen transport, Laser beam deflection technique, Diffusion-elastic phenomenon, Pd

1. Introduction

Hydrogen diffusion through hydride-forming electrodes such as Pd,[1] $LaNi_5$[2] and Zr-based alloy[3] accompanies the strain or stress field, which gives rise to a series of physical property change.[4-6] Knowledge of the stresses produced during hydrogen diffusion is of importance for the application of hydride-forming electrode to batteries, ion sensors and electrochromic devices.

However, there are few in-situ methods for measuring the stresses developed during hydrogen diffusion. Recently, laser beam deflection (LBD) technique has been successfully applied in our laboratory to explore the stresses generated during hydrogen diffusion through Pd foil and $Ni(OH)_2$ film electrodes under potentiostatic, self-discharge and potential scanning conditions.[7-11]

The purpose of this article is to overview the application of LBD technique to the analysis of the stress produced during hydrogen diffusion. For this purpose, we firstly explain the theoretical backgrounds of LBD technique; the elasto-diffusive and diffusion-elastic phenomena, a model for the diffusion-elastic phenomenon and secondly describe the experimental apparatus and two kinds of electrode specimen used for LBD technique. Finally, we present the analysis of the stresses generated during hydrogen extraction from Pd foil electrode in 0.1 M NaOH solution as example of LBD technique.

†E-mail: sipyun@mail.kaist.ac.kr

2. Theoretical Backgrounds

2.1. Elasto-diffusive phenomenon, Gorsky effect

The relationship between hydrogen diffusion and macroscopic deformation of the electrode specimen can be classified into the elasto-diffusive and diffusion-elastic phenomena,[12] which are indicated briefly in Table 1.

Fig. 1 shows the change in the hydrogen pressure within a $Pd_{81}Pt_{19}$ tubular membrane with time from an initial virtually value p_o, following an increase of hydrogen concentration of the outer surface at A. Preparatory to observation of the effect, initial condition of virtually constant pressures of hydrogen gas was established within the tubular membrane and the hydrogen gas was in equilibrium with hydrogen distributed over the tubular membrane. A subsequent increase of hydrogen concentration of the outer surface by increase of outer hydrogen pressure results in the initial decreases of the

Table 1. Elasto-diffusive and diffusion-elastic phenomena

Phenomenon	Original state	Primary cause	Consequence	Direction of flux (final state)
Elasto-diffusive	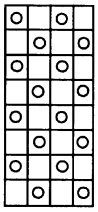	Elastic bending	Inhomogeneous hydrogen distribution	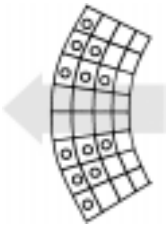
Diffusion-elastic	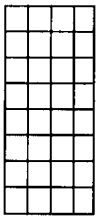	Diffusion flux	Inhomogeneous elastic deformation	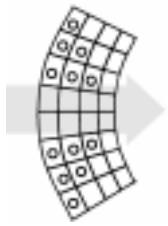

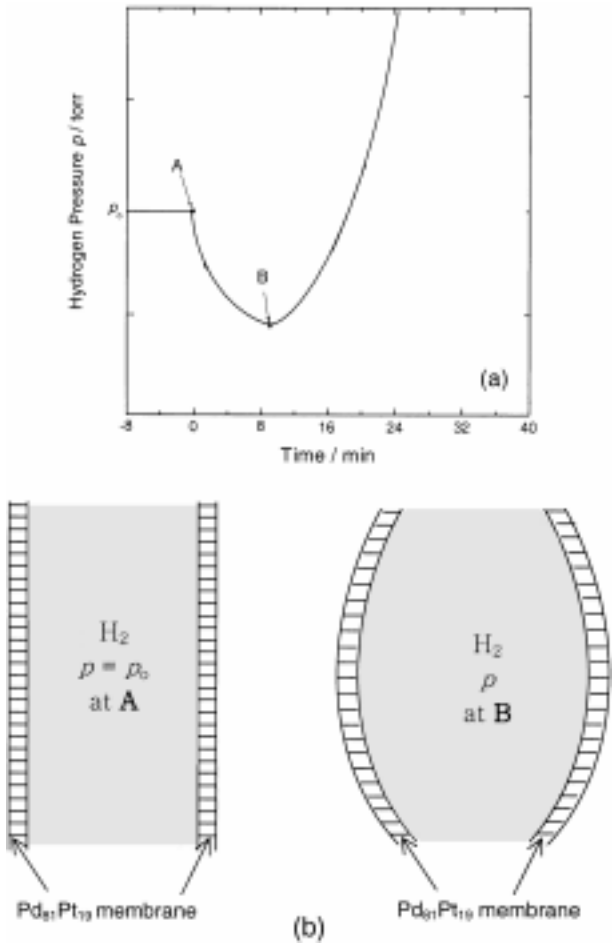

Fig. 1. (a) Change in hydrogen pressure within a $Pd_{81}Pt_{19}$ tubular membrane with time from an initial virtually constant pressure p_o of hydrogen gas, following an increase of hydrogen concentration of the outer surface at A. (b) Diagrammatic comparison of the shape of the tubular membrane at points A and B in (a).

hydrogen pressure within the tube (B in Fig. 1(a)).

This phenomenon is so small that one can hardly perceptible unless the inner surface of the tubular membrane is highly catalytically active for equilibration with the hydrogen gas contained within the tube. Such a sufficiently high surface activity can be satisfactorily achieved by electrolytically coating the inner surface with palladium black.[13-15)]

The causes of this effect have been identified with outward bending of the tubular membrane ensuing from expansion of the outer part of the tubular membrane, as illustrated in Fig. 1(b). The condition of outward bending of the tubular membrane produces hydrogen diffusion from regions close to the inner surface towards the outer surface. This phenomenon has been classified as the elasto-diffusive phenomenon, which is called "Gorsky effect".[13)] It has been known that the relative magnitudes of this phenomenon are related to the initial hydrogen concentration. Recently, by applying hydrogen permeation technique for tubular membranes of Pd and Pd-alloys, the stress field developed during Gorsky effect has been analysed in both experimental and theoretical aspects.[14-17)]

2.2. Diffusion-elastic phenomenon

The primary cause of the diffusion-elastic phenomenon is the hydrogen diffusion-flux resulting from the hydrogen concentration difference across the electrode specimen. The inhomogeneous hydrogen distribution causes an inhomogeneous dilation of crystal lattice of the electrode specimen, which gives rise to a bending of the electrode specimen if one-dimensional diffusion through the electrode is considered. The hydrogen flux is directed towards the concave surface.

It is important to appreciate that the bending distortions generated during hydrogen diffusion also induce the Gorsky effect. However, the analysis[18)] has indicated that any contributions of Gorsky effect to bending distortion should be lower by two orders in magnitude than contributions from the diffusion-elastic phenomenon and hence, it is reasonable to neglect the Gorsky effect in this work. The diffusion-elastic phenomenon is embodied in LBD technique.

2.3. Model for diffusion-elastic phenomenon

The initial condition (I.C.) in the electrode and boundary condition (B.C.) at the electrode surface are established during potentiostatic hydrogen extraction under the impermeable boundary condition as follows:

$$\text{I.C.} \quad c_H = c^o \qquad \text{for } 0 < x < L,\ t = 0 \tag{1}$$

$$\text{B.C.} \quad c_H = 0 \qquad \text{for } x = 0,\ t > 0 \tag{2}$$

$$\text{B.C.} \quad -F\tilde{D}_H\left(\frac{\partial c_H}{\partial x}\right) = 0 \qquad \text{for } x = L,\ t > 0 \tag{3}$$

where c_H is the hydrogen concentration; c^o, the equilibrium hydrogen concentration corresponding to the applied potential; L, the thickness of the electrode specimen; F, the Faraday constant; $\tilde{D}_H$, hydrogen diffusivity and x represents the distance from the electrolyte/electrode interface. In this respect, Fick's second law is employed as the governing equation for hydrogen diffusion:

$$\frac{\partial c_H}{\partial t} = \tilde{D}_H \frac{\partial^2 c_H}{\partial x^2}, \ (\tilde{D}_H \neq f(c_H),\ 0 < x < L) \tag{4}$$

On the other hand, the relative increase of volume of the elementary cell $\Delta V/V$ is proportional to c_H (Vegard's second law).[19]

$$\Delta V/V = k_3 c_H \tag{5}$$

where k_3 is proportionality coefficient of Vegard's second law. If $\Delta V/V$ is very small, the relative change of linear dimensions $\Delta l/l$ in the y-direction, obeys the same law of proportionality with a different coefficient, k_1.

$$\Delta V/V \ll 1 \quad \Delta l/l \equiv \varepsilon = k_1 c_H \tag{6}$$

Here, ε represents the linear strain, i.e., the relative deformation. Here, the y-axis is parallel to the longitudinal axis of the foil electrode specimen subjected to the diffusion-elastic phenomenon and perpendicular to the diffusion flux.

The distribution of stresses originating from the hydrogen concentration distribution across the electrode can be calculated by solving Hooke's law.

$$\sigma_y(x, t) = E\varepsilon(x, t) = k_1 E c_H(x, t) = k c_H(x, t) \tag{7}$$

where k is also proportionality coefficient.

The bending moment of the foil electrode specimen due to the inhomogeneous hydrogen distribution, $M_b(t)$, is given as

$$\begin{aligned} M_b(t) &= \int_0^L \sigma_y(x, t) \times \left(x - \frac{1}{2}\right) dx \\ &= \int_0^L k c_H(x, t) \times \left(x - \frac{1}{2}\right) dx \end{aligned} \tag{8}$$

Under the assumption that the change in $M_b(t)$ with time is proportional to the variation in deflection with time, we can calculate deflection transients by using Eq. (8) combined with the calculated hydrogen concentration profile transient. It should be stressed that hydrogen located in the region $0 < x < L/2$ contributes to the compressive deflection, whereas hydrogen residing in the region $L/2 < x < L$ does to the tensile deflection.

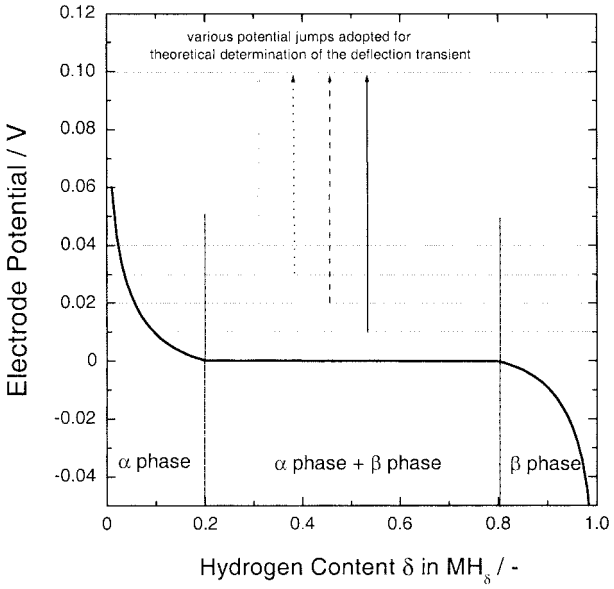

Fig. 2. Virtual electrode potential versus hydrogen content curve used for numerically analysing the deflection transient.

2.4. Deflection transient calculated under virtual electrode potential-hydrogen content curve

Fig. 2. depicts the virtual electrode potential curve versus hydrogen content. It should be noted that at a hydrogen extraction potential 0.10 V, the equilibrium hydrogen concentration is zero. The deflection transients theoretically calculated from the electrode in the presence of the single α phase are given in Fig. 3(a) at the potential jumps from various hydrogen injection potentials 0.01, 0.02, 0.03 and 0.04 V to 0.10 V as indicated in Fig. 2. Fig. 3(b) presents the change in the hydrogen concentration profile across the electrode with time in the presence of the single α phase at the potential jump of 0.01 to 0.10 V.

During hydrogen extraction, all tensile deflections drop to the maximum value and then are completely annihilated. The extracted hydrogen from the electrode produces the tensile stresses within the electrode, indicating that the extracted hydrogen contracts the lattice parameter of the electrode. The lower the preceding hydrogen injection potential is, the higher becomes the maximum value of the tensile deflection. However, the time to the maximum tensile deflection t_{max} has the same value, regardless of the preceding hydrogen injection potential.

Fig. 4 represents the variation in the deflection transient with hydrogen diffusivity. The deflection transients were calculated at the potential jump of 0.01 to 0.10 V with various hydrogen diffusivities. As hydrogen diffusivity is increased, the value of t_{max} is shortened, but the maximum of tensile deflection shares the same value. This indicates that the value of t_{max} depends strongly on hydrogen diffusivity $\tilde{D}_H$.

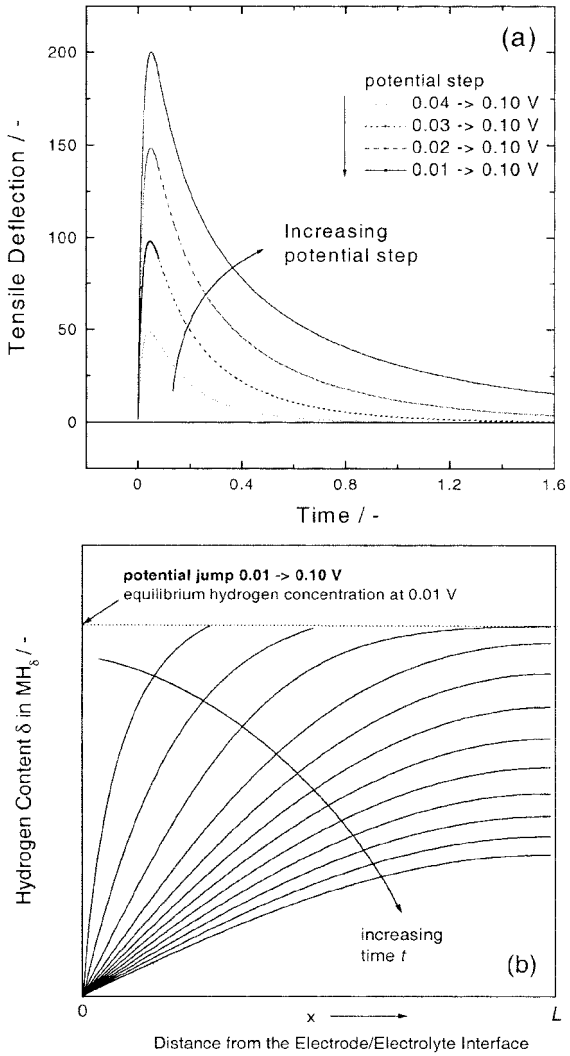

Fig. 3. (a) The calculated deflection transients at the potential jumps from various hydrogen injection potentials 0.01, 0.02, 0.03 and 0.04 V, to 0.10 V. (b) The simulated hydrogen concentration profile transient across the electrode at the potential jump of 0.01 to 0.10 V.

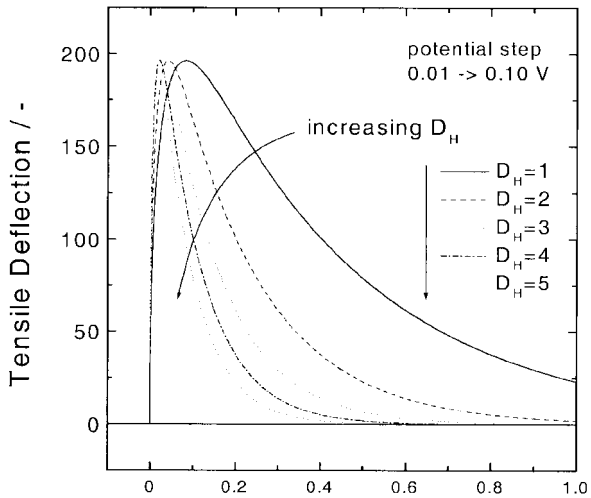

Fig. 4. Change in the deflection transient with hydrogen diffusivity. The deflection transients were calculated at the potential jump of 0.01 to 0.10 V with various hydrogen diffusivities.

The hydrogen concentration profile corresponding to the maximum tensile deflection can be specified by the dimensionless term $\tilde{D}_H t_{max}/L^2 = 0.05$.[20] Therefore, $\tilde{D}_H$ in the electrode can be determined from the measured values of t_{max} and the given value of L.

3. Experimental

3.1. Laser beam deflection (LBD) technique

LBD technique, developed by Stoney[21] and later modified by Nelson and Oriani,[22] was used to obtain the deflection generated during hydrogen transport through the electrode. Fig. 5 shows the experimental apparatus for LBD technique.

The spot size and maximum output of He-Ne laser (MELLES GRIOT) used in this work were 590 μm and 5 mW at 632.8 nm, respectively. Changes of stress on the electrode surface cause the electrode specimen to bend and its free end to move. To track this motion a laser beam was directed through a flat window in the side of the cell and reflected off the mirror near the end of the strip. The reflected beam from mirror near the end of Pd foil electrode is intercepted by a PSD (Position Sensitive Detector, Hamamatsu Photonics K.K.) as a measuring instrument. As the beam moves across the PSD, the position of light spot striking the PSD corresponds linearly to output voltage of PSD ranging from -10 V to 10 V. Calibration is achieved by pushing or pulling the free end of the electrode specimen with a glass rod attached to a micrometer.

3.2. Two kinds of specimen for LBD technique

Two kinds of electrode specimen have been generally used for LBD technique, which are demonstrated in Fig. 6. The specimen A has been employed to investigate the stresses developed during anodic oxidation of metal such as W[23,24] and Al,[25] electrodeposition[26] and hydrogen injection into

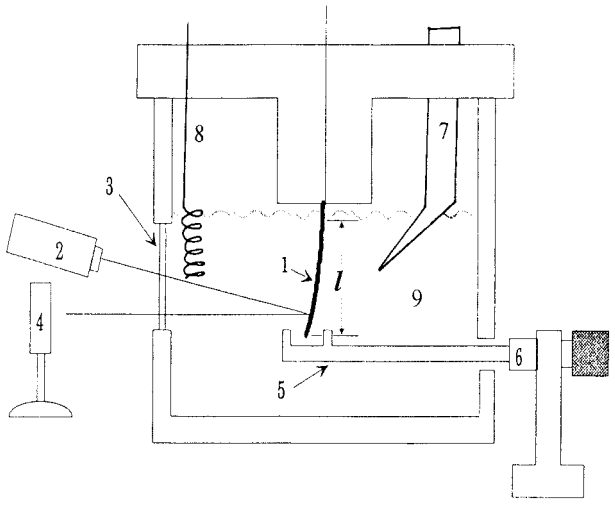

Fig. 5. Schematic view of the laser beam deflection experiment: 1, Specimen (working electrode); 2, He-Ne Laser source; 3, Flat window; 4, PSD (Position-Sensitive Detector); 5, Stainless steel rod; 6, Micrometer; 7, SCE (reference electrode); 8, Pt wire(counter electrode); 9, 0.1 M NaOH solution (electrolyte).

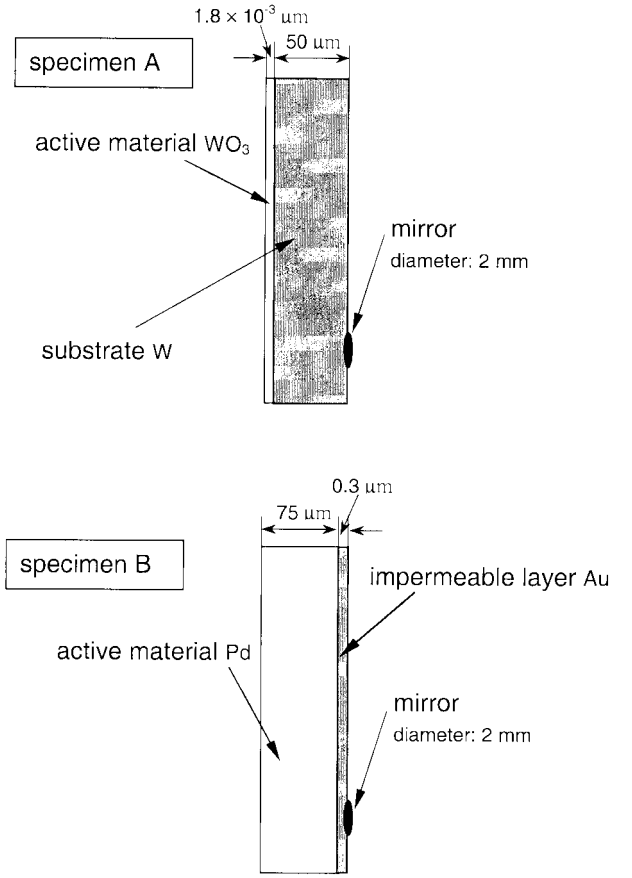

Fig. 6. Two kinds of electrode specimen used for the laser beam deflection technique.

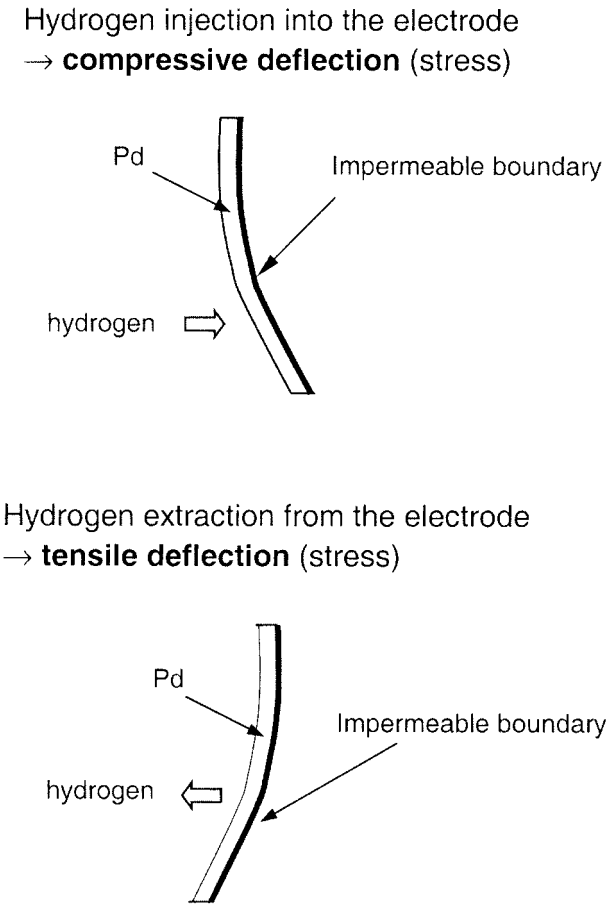

Fig. 7. Sign convention of the obtained deflection. (a) Hydrogen injection into the electrode: compressive deflection. (b) Hydrogen extraction from the electrode: tensile deflection.

WO_3 film electrode.[27] In this specimen, the thickness of active material is much thinner than that of substrate. For example, in the case of anodic oxidation of W, the thickness of active material and substrate are 1.8×10^{-3} and 50 μm, respectively. This specimen satisfies the plane stress condition. Thus, by using the Stoney equation,[21] the measured deflection can be quantitatively converted into the stress. However, the diffusion length for hydrogen is very short and consequently, this specimen is not appropriate for the analysis of the stresses generated during hydrogen diffusion through the electrode.

In contrast, in the specimen B, the thickness of active material (Pd foil electrode: 75 μm) is much greater than that of impermeable layer (Au layer: 0.3 μm) Therefore, this specimen can be effectively utilized to explore the stresses produced during hydrogen diffusion through the electrode. However, the deflection obtained from this specimen is not able to be quantitatively converted into the stress, because the active material is much thicker than Au layer, so that it satisfies the plane strain condition. It should be stressed that the measured deflection is simply proportional to be the generated stress.

In this work, the stresses developed during hydrogen diffusion through the electrode has been analysed by using the specimen B. Hydrogen injection into the active material causes the compressive stresses in the whole electrode specimen, while hydrogen extraction from the active material causes the tensile stresses in the whole electrode specimen. The sign convention of the obtained deflection is displayed in Fig. 7.

3.3. Specimen preparation and anodic current transient

The specimen was cut from 75 μm thick Pd sheet (Leico Co.) into foil with dimension of 3 mm × 90 mm. In order to remove residual stresses, the Pd foil specimen was annealed under a vacuum of 10^{-2} Pa at 650°C for 2 h, followed by furnace cooling. It was then mechanically ground with 1 μm alumina powder to eliminate surface oxide films. In order to make one side an impermeable boundary, a 0.3 μm thick Au layer was sputtered on one side of the electrode specimen. The other face of the foil electrode specimen was exposed (3 mm in width, 50 mm in length and 150 mm^2 in area) to the electrolyte.

A Pd foil electrode, a platinum wire and a saturated calomel electrode (SCE) were used as the working, counter and reference electrodes, respectively. An aqueous 0.1 M NaOH solution used as the electrolyte in this work was deaerated for 24 h by bubbling with purified argon gas before all electrochemical experiments. All potentials quoted

in this work are referred to a reversible hydrogen electrode (RHE), which was measured to be about -0.90 V(SCE) in 0.1 M NaOH solution (E(RHE) = E(SCE) + 0.90 V).[1)]

In order to activate the surface of Pd foil electrode and obtain the reproducible data, successive cyclic voltammetry was previously carried out in the potential range of -0.1 to 0.9 V(RHE) at a scan rate of 20 mV s^{-1}. Then, anodic current transients were measured on Pd foil electrode: the Pd foil electrode was first polarised at various hydrogen injection potentials -0.05, 0, 0.05 and 0.10 V(RHE) for 2×10^3 s. After that, hydrogen injection potential was jumped to 0.9 V(RHE) and from this moment on, the resulting anodic current and deflection were simultaneously recorded with time.

4. Results and Discussion

Fig. 8 illustrates the plot of electrode potential E against hydrogen content δ, obtained from the anodic current transient measured by jumping from various hydrogen pre-injection potentials -0.15 to 0.15 V(RHE) to a hydrogen extraction potential 0.90 V(RHE). Considering that the value of δ corresponding to E is equal to the amount of the anodic charge transferred during hydrogen extraction from the electrode, the value of δ was calculated by integrating the anodic current transient with respect to time. Here, we regard each pre-injection potential as E.

The tensile deflection is envisaged against time in Fig. 9. The deflection was measured from Pd foil electrode in 0.1 M NaOH solution by jumping various hydrogen injection potentials -0.05, 0, 0.05 and 0.10 V(RHE) to a hydrogen extraction potential 0.9 V(RHE), as indicated in Fig. 8. During hydrogen extraction, all tensile deflections drop to the maximum value and then are completely relaxed, irrespective of the preceding hydrogen injection potential. As the preceding

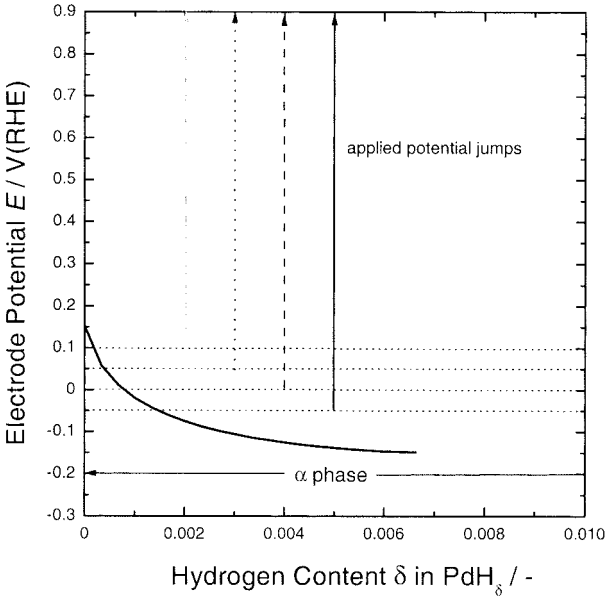

Fig. 8. Electrode potential E experimentally obtained from the Pd electrode in 0.1 M NaOH solution as a function of hydrogen content δ.

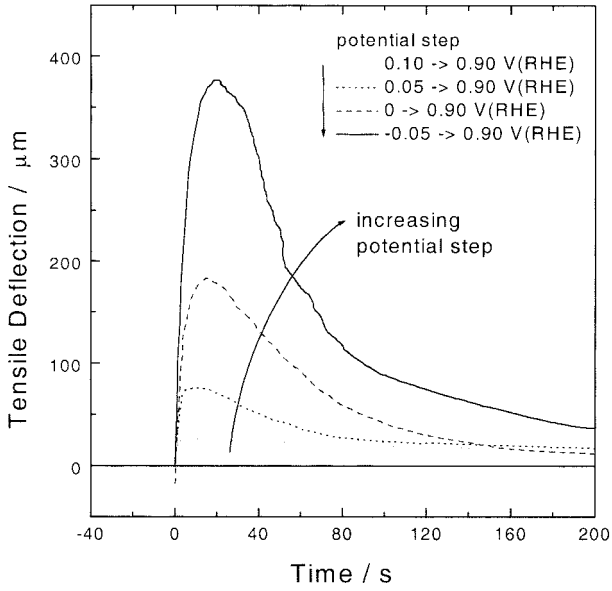

Fig. 9. Plot of tensile deflection against time, measured from Pd foil electrode in 0.1 M NaOH solution by jumping a hydrogen injection potential ranging from -0.05 to 0.10 V (RHE), to a hydrogen extraction potential 0.9 V(RHE).

hydrogen injection potential is decreased, i.e. the larger the amount of hydrogen injected into the Pd electrode is, the values of the maximum tensile deflection and t_{max} are increased.

It has no doubt that the difference between the molar volume of Pd at the electrolyte/electrode interface and that at the Au layer/electrode interface, which is caused by the extracted hydrogen, brings about the deflection of the specimen, i.e. the stresses. In this respect, it is reasonable to consider that the difference between the molar volume of Pd at the electrolyte/electrode interface and that at the Au layer/electrode interface is increased to the maximum value as hydrogen is extracted from the pre-charged Pd electrode. After that it begins to decrease as the concentration of hydrogen at the impermeable boundary is dropped below the equilibrium concentration.

Comparing the measured deflection transients in Fig. 9 with calculated deflection transients in Fig. 4 in terms of t_{max}, we can readily see that hydrogen diffusivity is diminished with decreasing preceding hydrogen injection potential. As the preceding hydrogen injection potential is decreased, hydrogen diffusivity determined during hydrogen extraction is decreased from 5×10^{-7} to 1×10^{-7} $cm^2 s^{-1}$, from the dimensionless term $\tilde{D}_H t_{max}/L^2$ = 0.05. These values of the hydrogen diffusivities are in good agreement with others.[1,28-30)]

5. Conclusion

The present work involves the application of LBD technique to the analysis of the stresses developed during hydrogen diffusion through Pd foil electrode. First, we briefly explain the elasto-diffusive (Gorsky effect) and diffusion-elastic phenomena, and describe the experimental appa-

ratus and two kinds of the electrode specimen used for LBD technique. Second, we theoretically derive a model for the diffusion-elastic phenomenon from the solution of the Fick's equation for given initial and boundary conditions, Vegard's second law and Hooke's law. The deflection transient is simulated as functions of applied potential step and hydrogen diffusivity to compare with the deflection transient measured from Pd foil electrode in 0.1 M NaOH solution. From the comparison between the deflection transient calculated and that measured, we finally explain the change in the tensile deflection with time in terms of the variation in the hydrogen concentration profile across the electrode with time and hydrogen diffusivity. From the experimental results, it turns out that LBD technique is effectively employed to analyse in-situ the stresses developed during hydrogen diffusion through the electrode.

Acknowledgements

The present work has been carried out under the auspices of the joint program of Korea Science and Engineering Foundation (KOSEF) and Japan Society for the Promotion of Science (JSPS) 1999/2001. The authors are indebted to KOSEF for the financial support of this work. Furthermore, this work was partly supported by the Brain Korea 21 project.

References

1. J.-N. Han, S.-I. Pyun and T.-H. Yang, *J. Electrochem. Soc.*, **144**, 4266 (1997).
2. C. Iwakura, T. Oura, H. Inoue, M. Matsuok and Y. Yamamoto, *J. Electroanal. Chem.*, **398**, 37 (1995).
3. X.-L. Wang, S. Suda and S. Wakao, *Z. Phys. Chem.*, **183**, 297 (1994).
4. H. Peisl, "Hydrogen in Metals I", (Edited by G. Alefeld and J. Völkl), 53, Springer-Verlag, Berlin (1978).
5. F. A. Lewis, K. Kandasamy and B. Baranowski, *Platinum Metals Rev.*, **32**, 22 (1988).
6. B. Baranowski, *J. Less-Common Metals*, **154**, 329 (1989).
7. J.-N. Han, S.-I. Pyun and D.-J. Kim, *Electrochim. Acta*, **44**, 1797 (1999).
8. J.-N. Han and S.-I. Pyun, *Electrochim. Acta*, **45**, 2781 (2000).
9. S.-I. Pyun, K.-H. Kim and J.-N. Han, *J. Power Sources*, **91**, 92 (2000).
10. J.-N. Han, M. Seo and S.-I. Pyun, *J. Electroanal. Chem.*, **499**, 152 (2001).
11. J.-N. Han, J.-W. Lee, M. Seo and S.-I. Pyun, press in *J. Electroanal. Chem.*, (2001).
12. J. Cermak and A. Kufudakis, *J. Less-Common Metals*, **49**, 309 (1976).
13. W.S. Gorsky, *Phys. Z. Sowjetunion*, **8**, 457 (1935).
14. F. A. Lewis, K. Kandasamy and B. Baranowski, *Platinum Metals Rev.* **32**, 22 (1988).
15. B. Baranowski, *J. Less-Common Metals*, **154**, 329 (1989).
16. K. Kandasamy, *Int. J. Hydrogen Energy*, **20**, 455 (1995).
17. Y. Sakamoto, H. Tanaka, F. A. Lewis, X. Q. Tong and K. Kandsamy, *Int. J. Hydrogen Energy*, **21**, 1025 (1996).
18. J. Cermak, A. Kufudakis and F.A. Lewis, *Z. Phys. Chem.*, **181**, 233 (1993).
19. J. Cermak and A. Kufudakis, *Czech. J. Phys. B.*, **23**, 1370 (1973).
20. J. Crank, "The Mathematics of Diffusion", 50, Oxford University Press, New York (1975).
21. G. G. Stoney, *Proc. Proy. Soc.*, **A82**, 172 (1909).
22. J. C. Nelson and R. A. Oriani, *Electrochim. Acta*, **37**, 2051 (1992).
23. S.-I. Pyun, J.-D. Kim and R.A. Oriani, *Mat. Sci. Forum.*, **185-188**, 407 (1995).
24. J.-D. Kim, S.-I. Pyun and R.A. Oriani, *Electrochim. Acta*, **41**, 57 (1996).
25. S.-M. Moon and S.-I. Pyun, *Electrochim. Acta*, **43**, 3117 (1998).
26. M.A. Butler and D.S. Ginley, *J. Electrochem. Soc.*, **134**, 510 (1987).
27. D.-J. Kim and S.-I. Pyun, *Electrochim. Acta*, **44**, 1723 (1999).
28. M. A. V. Devanathan and Z. Stachurski, *Proc. Roy. Soc.*, **270**, 90 (1962).
29. R. V. Bucur and F. A. Lewis, *Z. Phys. Chem.*, **181**, 209 (1993).
30. H. Ura, T. Nishina and I. Uchida, *J. Electroanal. Chem.*, **396**, 169 (1995).